Research article

# RIOK3 promotes pancreatic ductal adenocarcinoma cell invasion and metastasis by stabilizing FAK

Mengyuan Xu [a,b,1], Lei Fang [a,1], Xin Guo [a,c,1], Henan Qin [a], Rui Sun [a], Zhen Ning [a,c,**], Aman Wang [a,c,*]

[a] The First Affiliated Hospital of Dalian Medical University, Dalian Medical University, Dalian 116000, China
[b] Hangzhou Medical College Affiliated Lin'an People's Hospital, Hangzhou 310000, China
[c] Liaoning Key Laboratory of Molecular Targeted Drugs in Hepatobiliary and Pancreatic Cancer, Dalian 116000, China

## HIGHLIGHTS

- FAK activation is required for RIOK3 to promote PDAC cell invasion and metastasis.
- RIOK3 binds to and stabilizes the FAK protein.
- *RIOK3* is highly expressed in PDAC tissues and associated with poor prognosis.

## ARTICLE INFO

## ABSTRACT

Pancreatic ductal adenocarcinoma (PDAC) is an extremely aggressive cancer, characterized by a high metastatic burden. RIO Kinase 3 (RIOK3) has been shown to promote invasion and metastasis of PDAC by cytoskeleton remodeling, but the exact mechanism is still unknown. In this study, we analyzed transcriptome sequencing data from RIOK3 stable knockdown PANC-1 cells and TCGA-PDAC data and discovered that RIOK3 was substantially related to focal adhesion signaling in PDAC. Additionally, silencing RIOK3 dramatically decreased Focal Adhesion Kinase (FAK) protein expression and phosphorylation (Tyr397 and Tyr925 sites). Immunoprecipitation assay verified the interaction of RIOK3 and FAK. Furthermore, RIOK3 considerably increased the protein stability of FAK protein but not FAK-Y925F protein. The biological function of RIOK3 in increasing PDAC cell invasion and migration was shown to be dependent on FAK activation. Moreover, we discovered that *RIOK3* mutations were mainly characterized by amplification. *RIOK3* mRNA was found to be significantly elevated in PDAC tissues and was associated with a poor prognosis. Furthermore, *RIOK3* mRNA was significantly upregulated in later T-stage, pre-existing lymph node metastases, and later pathological stage samples. Overall, our study found that RIOK3 promotes PDAC cell invasion and metastasis by stabilizing FAK protein expression and upregulating its phosphorylation. This also provides a new target for therapeutic modalities targeting FAK.

## 1. Introduction

Pancreatic ductal adenocarcinoma (PDAC) accounts for more than 90% of pancreatic cancers, and it is the fourth leading cause of cancer-related deaths in the United States in 2020, with a 5-year survival rate of only 10% [1]. The majority of patients are already advanced at diagnosis, with a median survival of only 6–10 months. This low survival rate is a result of PDAC's proclivity for metastasis and the ineffectiveness of cytotoxic, targeted, and immunotherapy.

RIO Kinase 3 (RIOK3) is a member of the RIO family, which includes RIO Kinase 1 (RIOK1), RIO Kinase 2 (RIOK2) and RIOK3, and is primarily involved in ribosome synthesis and processing. The deletion of RIOK3 resulted in an increase in the level of pre-21S rRNA in the 18S rRNA production pathway [2]. Additionally, RIOK3 was found to regulate the type I interferon pathway during viral infection [3, 4]. In recent years,

the role of RIOK3 in tumorigenesis has been initially explored, and it was found that RIOK3 promotes the proliferation, migration and invasion of a variety of solid tumor cells. Furthermore, RIOK3 has been found to promote invasion and metastasis of PDAC and breast cancers through cytoskeleton remodeling [5, 6, 7], but the exact mechanism remains unclear. Our bioinformatic analysis of The Cancer Genome Atlas (TCGA)-PDAC data demonstrated that RIOK3 had the highest mutation rate in the RIO family, at 14%, and was mostly characterized by amplification, whereas *RIOK1* and *RIOK2* had low mutation rates of 0.6 % and 0 %, respectively. This increased our focus on RIOK3. In this study, we observed that RIOK3 interacts with Focal Adhesion Kinase (FAK) in PDAC cells and enhances PDAC cell invasion and metastasis by stabilizing FAK protein expression.

## 2. Materials and methods

### 2.1. Cell culture and reagents

The human PDAC cell lines PANC-1, BxPC-3 and HEK293T cells were obtained from the Cell Bank of the Chinese Academy of Sciences (Shanghai, China), and were cultured in DMEM (GIBCO, USA) for PANC-1 and HEK293T cells or RPMI 1640 (GIBCO, USA) for BxPC-3 cells. Cell lines were maintained in culture supplemented with 10% FBS (GIBCO, USA) and 1% penicillin/streptomycin (Thermo, USA) at 37 °C with 5% $CO_2$ in a humidified incubator (Thermo, USA).

The following antibodies and reagents were used: anti-RIOK3 (A305-601A-T, Thermo, USA), anti-FAK (71433S, CST, USA), anti-Phospho-FAK
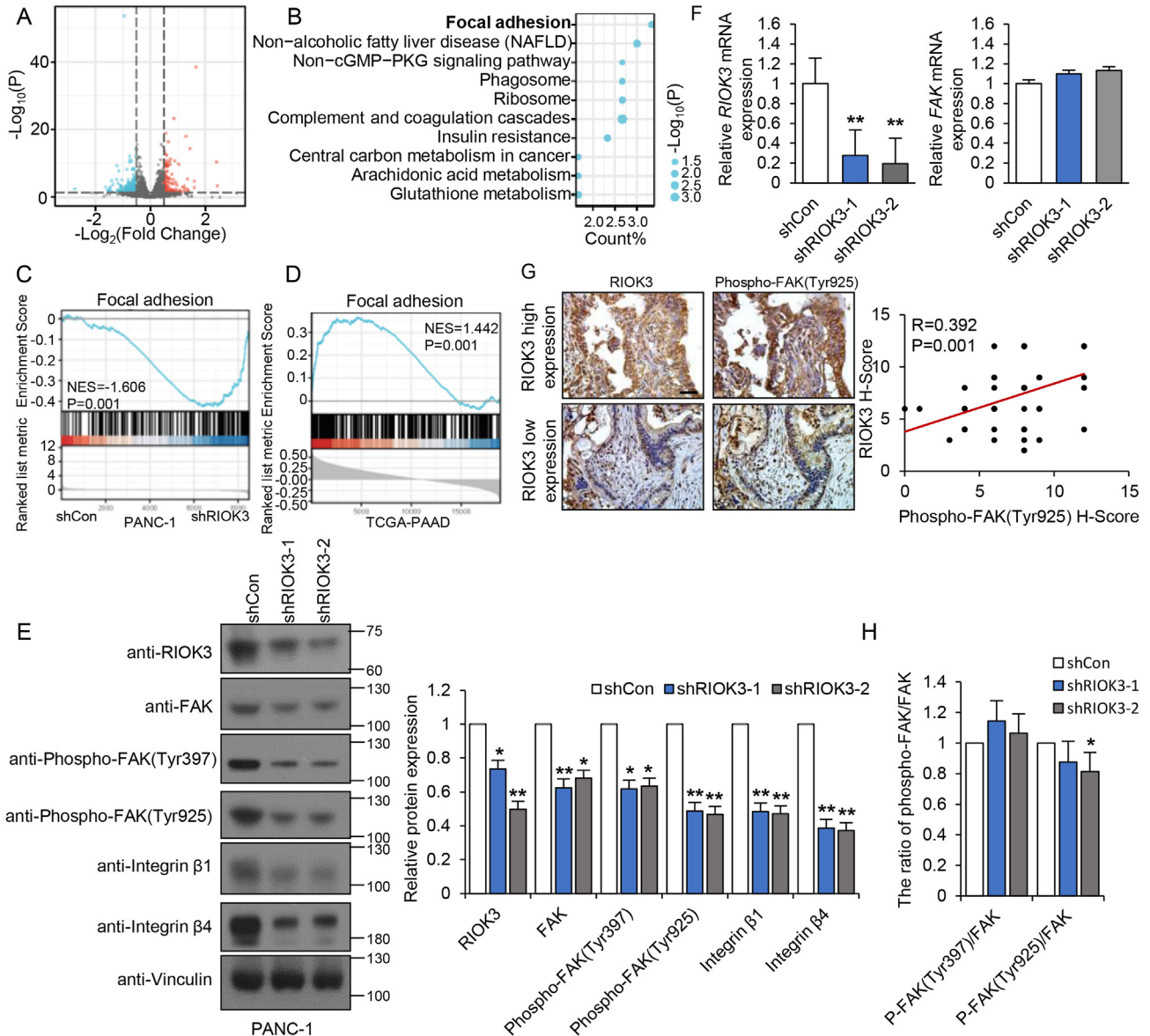


**Figure 1.** Knockdown of RIOK3 significantly inhibits FAK activation in PDAC cells. Using lentiviral transfection, PANC-1 cells with stable knockdown of RIOK3 were created, followed by RNA extraction and sequencing. Up-regulated (red) and down-regulated (blue) mRNAs were characterized using volcano plots (A). Differential genes (| Log2FC | > 0.5, FDR ‹ 0.05) were used to perform a KEGG pathway enrichment analysis (B). The Log2 FC of all mRNA expression was used in GSEA (C). The spearman correlation coefficients of *RIOK3* with all other genes in the TCGA-PDAC transcriptome database were used in GSEA (D). Western blot assay and quantitative analysis of the protein expression of RIOK3, FAK, Phospho-FAK(Tyr397), Phospho-FAK(Tyr925), Integrin 1, Integrin 4, and vinculin in cells (E). The qRT-PCR method was used to detect *RIOK3* and *FAK* mRNA expression (F). Representative IHC staining of RIOK3 and Phospho-FAK(Tyr925) in pancreatic cancer tissues and correlation analysis between RIOK3 and Phospho-FAK(Tyr925) based on H-Score (G). R represents Pearson correlation coefficient. Analysis of the ratio of phospho-FAK/FAK in Figure 1E (H). The data shown represent the means (±SD) of biological triplicates. *p < 0.05, **p < 0.01, ANOVA test. The uncropped images of (E) were referred to in supplementary Figure 1.

(Tyr397) (8556, CST, USA), anti-Phospho-FAK (Tyr925) (3284, CST, USA), anti-Phospho-FAK (Tyr925) (AF3619, Affinity Biosciences, USA), anti-Integrin β1 (9699, CST, USA), anti-Integrin β4 (14803, CST, USA), anti-Integrin β5 (3629, CST, USA), anti-MYC Tag (60003-2-Ig, Proteintech, China), anti-Vinculin (SC-73614, Santa Cruz Biotechnology, USA) and cycloheximide (CHX Inalco Spa Milano Italy).

## 2.2. Plasmids

Lentiviral shRNAs were cloned in pLKO.1 within the AgeI/EcoRI sites at the 3′end of the human U6 promoter. The targeted sequences were: shRIOK3-1:5′-CTGTT GTCT TTCATGCATATG-3′; shRIOK3-2 5′-GTTGCGTCTTTCCTTGAATAT-3′. shFAK-1: 5′-CCAGGGATTATGA-GATTCAAA-3′.

All expression vectors utilized in this work were produced utilizing Gateway Technology, including HA-RIOK3, Myc-FAK and pLoc-HA-RIOK3. Briefly, cDNAs encoding attB homologs were produced by PCR and subsequently subcloned into the pDONR221 vector as entry clones. The entering clones were then recombined into gateway destination vectors with various tags (HA and Myc) or lentiviral vectors (pLoc). For the Myc-FAK-Y925F vector, an overlap extension PCR was used to create a mutation in the FAK cDNA, which was subsequently cloned into the Myc vector.

## 2.3. Construction of stable transfected cell lines

$2 - 3 \times 10^7$ HEK293T cells were grown in a 10 cm culture dish and Lipofectamine 2000 was used to co-transfect the plasmid with psPAX2 and pVSVG according to the manufacturer's instructions. 48 hours after transfection, condition media containing recombinant lentiviruses was collected and filtered using non-pyrogenic filters with a pore size of 0.45 μm (Merck Millipore, Billerica, MA, USA). Supernatants from these samples were immediately administered to target cells along with Polybrene (Sigma-Aldrich, St. Louis, MO, USA) at a final concentration of 8 mg/ml, and the supernatants were incubated with the cells for 12 h. Following infection, cells were grown in fresh growth media as usual. 48 hours after infection, selection with 2 g/ml puromycin (InvivoGen) or 8 g/ml blasticidin (InvivoGen) was commenced.

## 2.4. Migration and invasion assays

Transwell chambers (8 μm pore size; Corning Co., NY) were used in the *in vitro* migration assay. After transfection, cells were seeded in upper chamber at a cell density of $1 \times 10^5$ with lower chamber supplied with complete culture medium. 24 h later, invaded cells to bottom were fixed for staining in crystal violet solution, followed by observation under microscope. Three random fields of each membrane were imaged and the number of migrating cells counted. Similar inserts coated with Matrigel were used to determine the invasive potential.

## 2.5. Western blot

Western blot analysis was performed with standard methods [8]. Briefly, cells were lysed in radio immunoprecipitation assay (RIPA) buffer containing protease inhibitors (Sigma, St. Louis, MO, USA) and phosphatase inhibitors (Roche, Sigma, St. Louis MO, USA). Proteins were separated by sodium dodecyl sulfate-polyacrylamide gel electrophoresis (SDS-PAGE) and blotted onto a PVDF membrane (Bio-Rad, Hercules, CA, USA). Membranes were probed with specific primary antibodies at 4 °C overnight and then with peroxidase-conjugated secondary antibodies. Equal protein-sample loading was monitored using Vinculin antibody. The bands were visualized by chemiluminescence or film (BOTHCATKIN X-ray Film Processor, P14-A).

## 2.6. Co-immunoprecipitation (Co-IP) assay

In brief, the cells were lysed by incubation with 600 μL lysis buffer and Protease & Phosphatase Inhibitor Cocktail at 4 °C for 30 min,

followed by centrifugation at 13500 g for 15 min. The supernatant was harvested and a small aliquot was reserved as the input group. The remaining samples were divided into two tubes: one was incubated with 2 μg anti-RIKO3 and the other, acting as a negative control, was incubated with 2 μg of IgG (Beyotime, Shanghai, China). After incubation at 4 °C for 6 h, 30 μL of protein A/G (Thermo Fisher Scientific) was added to the mixture and incubated on a rotator overnight at 4 °C. After washing, bead-bound proteins were eluted by denaturing in an appropriate amount of protein loading buffer at 95 °C for 5 min and centrifuged; the supernatant was used for Western blot analysis.

## 2.7. Protein stability assay

After transfection, cells were treated with CHX (10 mg/ml) for the indicated durations before collection.

## 2.8. RNA isolation and quantitative real-time PCR

Trizol reagent (Takara, 9109, China) was used to isolate RNA from tumour cells. Concentration of RNAs were measured by Microplate Reader (BioTek, CYT5MFV, America). Absorbance OD 260nm/OD 280nm of RNAs are all in standard scale value (1.8–2.0). Reverse transcription PCR was performed using the Revert Aid First Strand cDNA synthesis kit (Fermentas; K1622 Thermo Fisher Scientific, Inc.) according to the protocol. Quantitative real-time PCR was carried out on a CFX96 instrument (Bio-Rad Laboratories, Hercules, CA, USA) using StepOnePlus and the DNA double-strand-specific reagent SYBR-Green I for detection (Roche Applied Science, Penzberg, Germany). All relative gene expression levels were measured by three biological replicates for different experimental groups and with three technical replicates per biological replicate. The relative expression levels of RNAs were calculated using the $2^{-\triangle\triangle}$Ct method after normalization to the ACTB expression. The Cq technique was used to calculate fold changes. All experimental designs and methods were followed MIQE guidelines. The sequences of the primers were:

*RIOK3:*

F 5′- AATATGATGCACAGCTTAGGCG -3′
R 5′- ATCACGAGTATCCTGCCAGTC -3′

*FAK:*

F 5′- GCTTACCTTGACCCCAACTTG -3′
R 5′- ACGTTCCATACCAGTACCCAG -3′

*ACTB:*

F 5′- CATGTACGTTGCTATCCAGGC -3′
R 5′- CTCCTTAATGTCACGCACGAT -3′

## 2.9. RNA sequencing

The RNeasy Mini kit (Qiagen) was used to extract RNA from PANC-1 cells according to the manufacturer's instructions. The Qubit 2.0 Fluorometer (Life Technologies, Carlsbad, CA, USA) was used to quantify RNA samples, and the 4200 TapeStation was used to assess RNA integrity (Agilent Technologies, Palo Alto, CA, USA). Technical staff from Hangzhou KaiTai Bio-lab performed the RNA sequencing and library creation.

## 2.10. Immunohistochemistry

The PDAC tissues microarrays (HPanA120Su02) were obtained from Shanghai Outdo Biotech Company (Shanghai, China). The experiments were approved by Research ethics committee at Shanghai Outdo Biotech Company. Standard IHC staining procedures were performed according to the instructions of IHC Kit (PK10006, Proteintech, USA). RIOK3
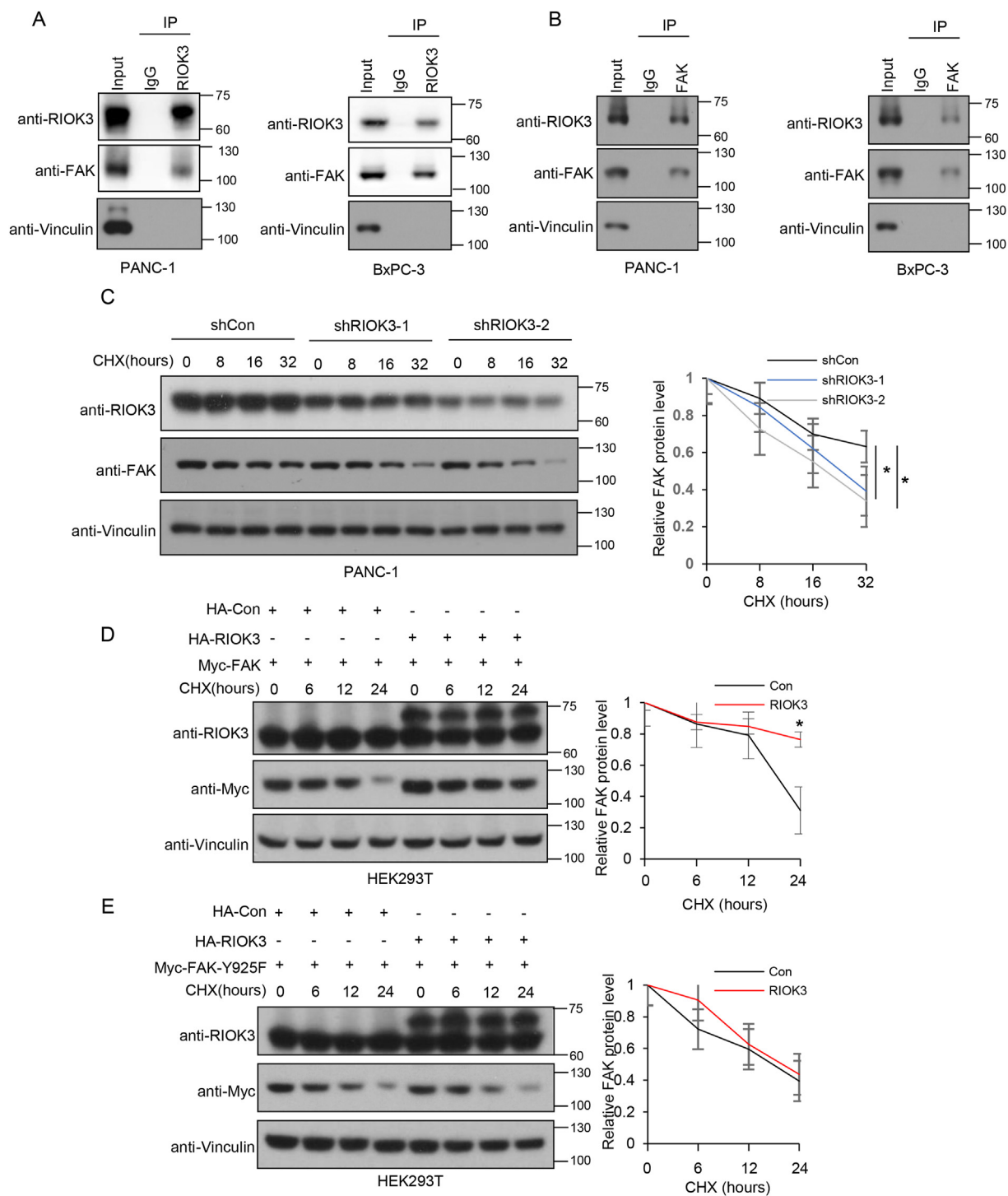
**Figure 2.** RIOK3 binds to and stabilizes the FAK protein. Co-IP assays were performed using RIOK3 antibody or IgG in protein lysates of PANC-1 cells and BxPC-3 cells, followed by western blot assays with RIOK3 and FAK antibodies (A). Co-IP assays were performed using FAK antibody or IgG in protein lysates of PANC-1 cells and BxPC-3 cells, followed by western blot assays with RIOK3 and FAK antibodies (B). A protein stability assay was used to test the stability of FAK protein in PANC-1-shRIOK3 cells (C). In HEK293T cells, HA-RIOK3 and Myc-FAK or Myc-FAK-Y925F were co-transfected, and the protein stability of Myc-FAK or Myc-FAK-Y925F was tested using a protein stability assay (D and E). The data shown represent the means ($\pm$SD) of biological triplicates. *p $<$ 0.05, **p $<$ 0.01, Student's t-test (unpaired, two-tailed) or ANOVA test. The uncropped images of (A and B) were referred to in supplementary Figure 2 and the uncropped images of (C, D and E) were referred to in supplementary Figure 3.

(A305-601A-T, Thermo, USA) (1:400) ang anti-Phospho-FAK (Tyr925) (AF3619, Affinity Biosciences, USA) (1:100) antibodies were applied as the primary antibodies in this study. Citrate solution was used for antigen retrieval depend on antibody instruction. H-score was used to assess the staining intensity. The intensity was scored as follows: 0, negative; 1, weak; 2, moderate; and 3, strong. The frequency of positive cells was

defined as follows: 0, less than 5%; 1, 15%–25%; 2, 26%–50%; 3, 51%–75%; and 4, greater than 75%. The H-Score (values, 0–12) was determined by multiplying the score for staining intensity with the score for positive area. When the staining was heterogeneous, we scored it as follows: each component was scored independently and summed for the results.

### 2.11. GSEA and KEGG pathway enrichment analysis

Spearman correlation coefficients were calculated between RIOK3 and all the other genes based on the RNA-seq expression matrix of the TCGA-PDAC tumor tissues. Then, the genes were ranked based on the correlation coefficients and utilized as the input for the gene set enrichment analysis (GSEA) based pathway enrichment analysis. The transcriptome data of the RIOK3 stable knockdown cells were dependent on the $Log_2$ Fold Change (FC) of mRNA expression for GSEA. Significantly different genes (Log2FC > 1, Q ᐸ 0.05) in the transcriptome data of the RIOK3 stable knockdown cells were subjected to KEGG pathway enrichment analysis using the website https://david.ncifcrf.gov/. GSEA was performed by the clusterProfiler R package. Pathway information was obtained from the Kyoto Encyclopedia of Genes and Genomes (KEGG, https://www.kegg.jp/) database.

### 2.12. Statistical analysis

To compare the means of more than two groups, an ANOVA-post-hoc pairwise comparison analysis was used. The mean value of two groups was compared using the Student's t-test (unpaired, two-tailed). The Kaplan-Meier test was used to calculate the differences in survival. The Pearson correlation coefficient was used to evaluate the relationship between RIOK3 and Phospho-FAK(Tyr925) protein expression levels in human PDAC tissues. After doing the Shapiro-Wilk normality test and Levene's test on the TCGA data, the independent sample t-test or Wilcoxon rank sum test was used. Bars and error represent mean ± standard deviations (SD) of replicate measurements. *p ᐸ 0.05, **p ᐸ 0.01 were used to indicate statistical significance. The SPSS 18.0 software package was used for statistical analysis (SPSS, Inc., Chicago, IL, USA).

## 3. Results

### 3.1. Knockdown of RIOK3 significantly inhibits FAK activation in PDAC cells

To explore the specific mechanisms by which RIOK3 promotes PDAC invasion and metastasis, we constructed PDAC cell lines with stable knockdown of RIOK3 and performed transcriptome sequencing (Figure 1A). We found that 184 genes were significantly down-regulated ($Log_2FC < -0.5$) with RIOK3 knockdown, and 33 genes were more than 2-fold down-regulated ($Log_2FC < -1$). Another 126 genes were significantly upregulated ($Log_2FC > 0.5$), including 23 genes with more than a 2-fold upregulation (Figure 1A). The KEGG pathway enrichment analysis of these differentially expressed genes revealed a significant association between RIOK3 and focal adhesion (Figure 1B). Subsequent GSEA confirmed that the Focal adhesion pathway was significantly down-regulated after RIOK3 knockdown (NES = −1.606) (Figure 1C). To validate this result, we performed a GSEA based on the TCGA PDAC database, which confirmed that RIOK3 was significantly positively correlated with focal adhesion (NES = 1.442) (Figure 1D). FAK is the critical component of focal adhesion, and we observed that silencing RIOK3 drastically decreased FAK protein expression and phosphorylation at the Tyr 397 and 925 sites
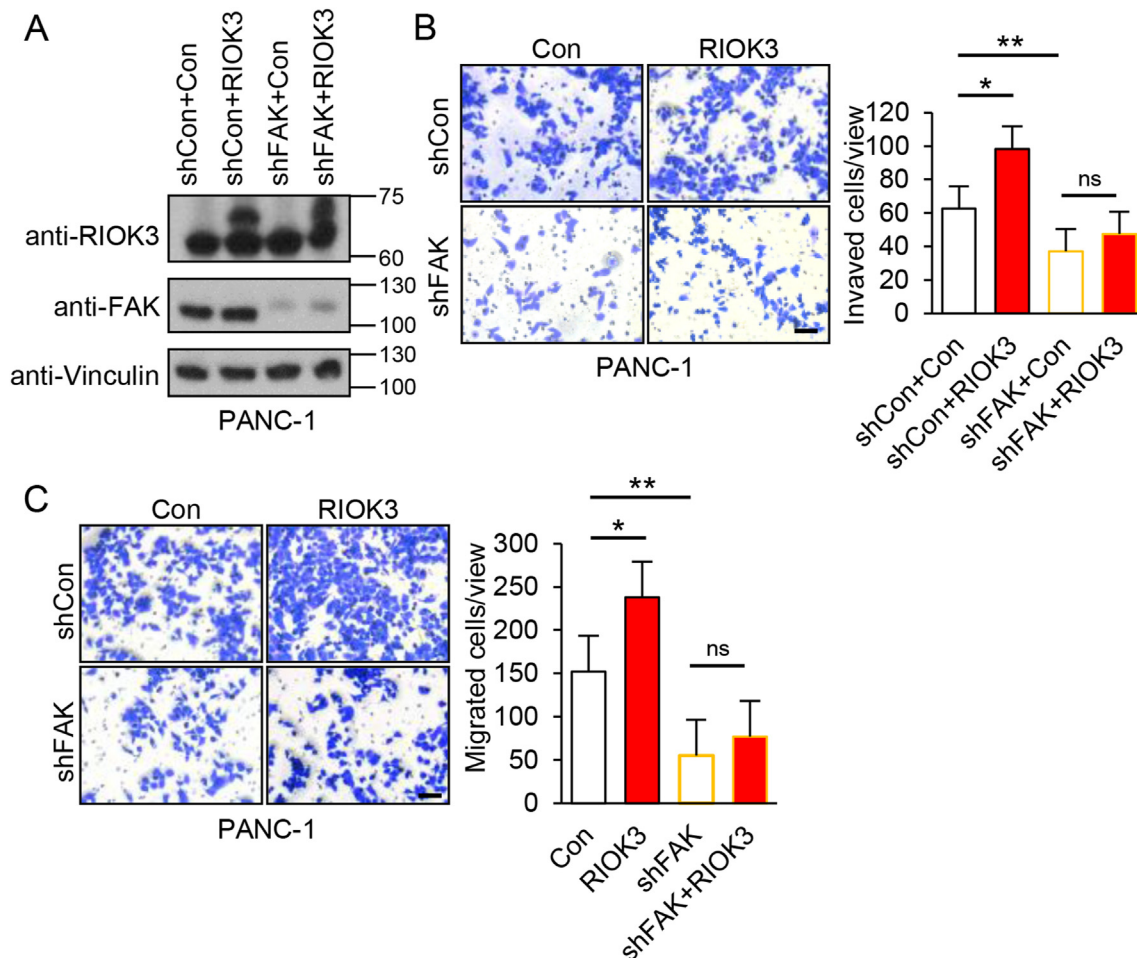


**Figure 3.** RIOK3 promotes invasion and metastasis of PDAC cells via FAK. PANC-1 cells overexpressing RIOK3 following FAK knockdown were constructed using lentiviral transfection, and the protein expression of RIOK3, FAK, and vinculin was determined using Western blot (A). The invasion (B) and migration (C) ability of the above cell lines was determined using the migration and invasion assays, respectively. Bar = 50μm. The data shown represent the means (±SD) of biological triplicates. *p < 0.05, **p < 0.01, ns, nonsignificant, ANOVA test. The uncropped images of (A) were referred to in supplementary Figure 4.

(Figure 1E), but had no effect on *FAK* mRNA (Figure 1F). Additionally, integrin β1/β4/β5 protein expressions were considerably reduced (Figure 1E). Subsequent IHC assays confirmed a significant positive correlation between the protein expression of RIOK3 and Phospho-FAK (Tyr925) in PDAC tissues (Figure 1G). Finally, we calculated the ratio of phospho-FAK/FAK and found no significant change in Phospho-FAK(Tyr397)/FAK after stable knockdown of RIOK3, but Phospho-FAK(Tyr925)/FAK was downregulated (Figure 1H). In summary, these data indicate that silencing RIOK3 dramatically decreased the protein expression and phosphorylation of FAK in PDAC cells.

### 3.2. RIOK3 binds to and stabilizes the FAK protein

FAK protein expression was dramatically decreased following RIOK3 knockdown, while mRNA expression remained unchanged. We

hypothesized that RIOK3 might have an effect on the stability of the FAK protein. Co-IP assays indicated that RIOK3 interacted with FAK in PDAC cells (Figure 2A and 2B). Subsequent FAK protein stability assay demonstrated that RIOK3 significantly increased the protein stability of FAK (Figure 2C and 2D). A previous study established that phosphorylating the FAK Tyr925 site increases the interaction of FAK with aB-crystallin and stabilizes the FAK protein [9]. To investigate whether the phosphorylation of the Tyr925 site, which is suppressed by RIOK3 knockdown, is linked with the decrease in FAK protein stability, we used a point mutation approach to replace Tyr-925 with a non-phosphorylated phenylalanine (FAK-Y925F). Then, HA-RIOK3 was co-transfected with Myc-FAK-Y925F in 293T cells and a protein stability assay was performed. The results indicated that RIOK3 had less effect on the protein stability of Myc-FAK-Y925F protein (Figure 2E). In summary, our findings indicate that RIOK3 interacts with and stabilizes FAK proteins,
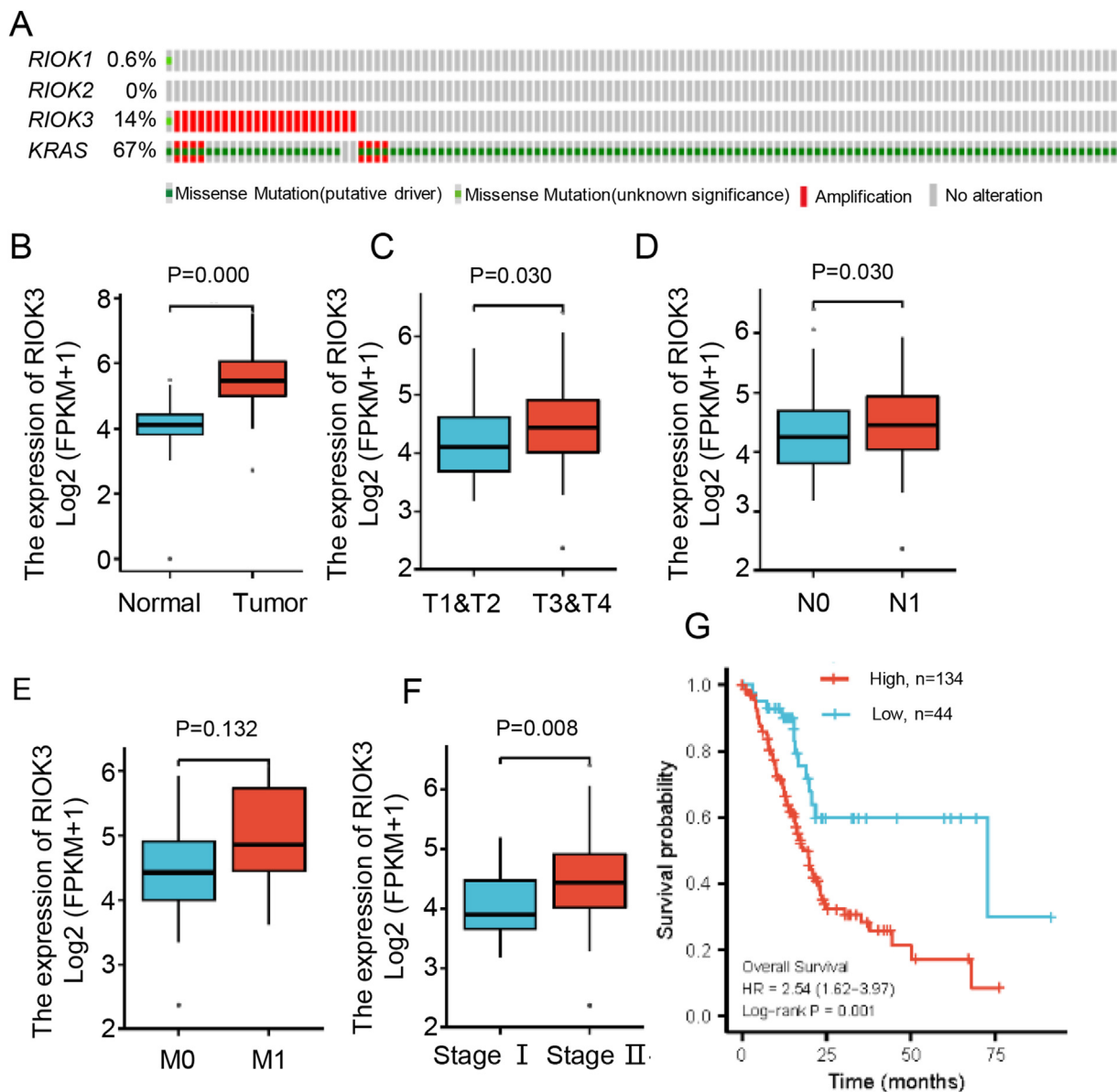


**Figure 4.** Mutation characterization, mRNA expression and correlation with prognosis of *RIOK3* in TCGA-PDAC database. The mutation rates and mutation characteristics of RIO family members (*RIOK1*, *RIOK2* and *RIOK3*) and *KRAS* in TCGA-PDAC genomic database were analyzed using online resources (http://www.cbioportal.org/index.do) (A). The expression of *RIOK3* mRNA in PDAC tissues and normal pancreatic tissues was analyzed using transcriptome data from the TCGA and GTEx datasets (Wilcoxon rank sum test) (B), Using TCGA-PDAC transcriptome data, we investigated the expression of *RIOK3* mRNA in different T-stage samples (T1&2 vs. T3&4) (independent sample t-test) (C), different N-stage samples (N0 vs. N1) (Wilcoxon rank sum test) (D), different M-stage samples (M0 vs. M1) (independent sample t-test) (E), and different pathological stage samples (Stage 1 vs. Stage 2–4) (independent sample t-test) (F). Kaplan–Meier curves of the survival analysis of *RIOK3*-positive patients based on the prognosis data of TCGA PDAC database (high = 134, low = 44) (G). *p < 0.05, **p < 0.01.

which may be related to RIOK3-mediated FAK Tyr-925 site phosphorylation.

### 3.3. RIOK3 promotes invasion and metastasis of PDAC cells via FAK

To further elucidate whether FAK is involved in RIOK3-induced PDAC invasion and metastasis, we overexpressed RIOK3 in cells with stable FAK knockdown (Figure 3A). Migration and invasion assays confirmed that RIOK3 overexpression significantly promoted PDAC cell invasion and metastasis. However, silencing FAK effectively reduced this tendency (Figure 3B and 3C). Overall, *in vitro* experiments confirmed that FAK plays a critical role in RIOK3-promoted invasion and metastasis.

### 3.4. RIOK3 is highly expressed in PDAC tissues and associated with poor prognosis

To determine whether RIOK3 is involved in PDAC progression, we first analyzed the mutation characteristics of RIO family members in the TCGA-PDAC database. We discovered that while *RIOK1* and *RIOK2* had mutation rates of only 0.6 % and 0 %, respectively, *RIOK3* had a mutation rate of 14 % and was predominantly amplified (Figure 4A). Subsequent analysis of PDAC transcriptome data from the TCGA and GTEx found that *RIOK3* mRNA expression was significantly increased in PDAC tissues as compared to normal tissues (Figure 4B). In addition, *RIOK3* mRNA expression was significantly upregulated in T stage 3–4 samples (Figure 4C), N1 stage samples (Figure 4D), and pathological stage 2–4 samples (Figure 4F) compared to T stage 1–2 samples, N0 stage samples, and pathological stage 1 samples. Although the difference in *RIOK3* mRNA expression between M1 and M0 samples was not statistically significant, it was still evident that *RIOK3* mRNA was increased in M1 samples than in M0 samples (Figure 4E), which may be accounted for the lower number of patients in the M1 group. Finally, we evaluated the prognostic value of *RIOK3* in this TCGA PDAC dataset. Of note, patients with high levels of *RIOK3* had much shorter overall survival than patients with low levels of RIOK3 (Figure 4G). Overall, our results confirm that high expression of *RIOK3* may be associated with the progression of PDAC.

## 4. Discussion

In this study, we discovered that RIOK3 promotes PDAC invasion and metastasis via activating FAK signaling. RIOK3 interacts with FAK and increases its protein stability, which may be associated with phosphorylation of the Tyr925 site of FAK protein.

Focal adhesion is a macromolecular complex that mediates cell-extracellular matrix (ECM) interactions by integrin receptors attached to the actin cytoskeleton via adhesion-associated proteins to regulate cellular ECM responses [10]. FAK is a critical component of focal adhesion. It is a cytoplasmic tyrosine kinase involved in cell proliferation, cytoskeletal remodeling, and signal transduction [11]. When integrins interact with the ECM, FAK is auto-phosphorylated at Tyr397, forming a high-affinity docking site for numerous proteins, including the Phosphoinositide 3-kinase (PI3K) p85 subunit and Src kinase. Src activation then phosphorylates numerous additional FAK sites, including Tyr925. Phosphorylation of the FAK Tyr397 and Tyr925 sites results in the formation of a binding site for the Growth factor receptor-bound protein 2 (Grb2)-son of sevenless (SOS) complex, which then sends a signal to the RAS- mitogen-activated protein kinase (MAPK) cascade [12]. Our study discovered a substantial association between RIOK3 and focal adhesion in PDAC. RIOK3 silencing dramatically decreased FAK protein expression and phosphorylation at the Tyr 397 and 925 phosphorylation sites. It was demonstrated that phosphorylating the FAK Tyr925 site enhances FAK's interaction with aB-crystallin and stabilizes FAK protein [9]. In this study, we found that RIOK3 was able to stabilize FAK proteins, but had less effect on FAK proteins with the Y925F mutation. This also suggests

that the stabilizing effect of RIOK3 on FAK proteins may be dependent on the phosphorylation of Tyr925.

The activation of FAK has been demonstrated to be critical in a variety of solid tumors [13, 14, 15, 16, 17], including PDAC. Pharmacological inhibition of FAK can result in lower stromal density in PDAC models, enhancing tumor response to chemotherapy and immunotherapy [18]. Several FAK inhibitors are now undergoing clinical studies [19]. In this study, we found that FAK knockdown significantly inhibited the invasion and metastasis of PDAC cells promoted by RIOK3 overexpression. This also implies that the pro-invasive effect of RIOK3 on PDAC is dependent on FAK activation. Subsequently, we found that *RIOK3* mRNA was significantly up-regulated in PDAC tissues. In addition, *RIOK3* in the genome was also characterized by amplification as the main mutation. Importantly, high expression of RIOK3 was significantly associated with poor prognosis in patients with PDAC. This also provides further evidence that RIOK3 may play an important role in the progression of PDAC.

In summary, this study has provided critical insights into the specific mechanisms of RIOK3 in PDAC invasion, revealed the critical position of FAK in the pro-tumor function of RIOK3, and provided a new potential strategy for targeting FAK therapy.

## Declarations

### Author contribution statement

Mengyuan Xu: Performed the experiments; Analyzed and interpreted the data.

Lei Fang; Xin Guo: Performed the experiments; Analyzed and interpreted the data; Contributed reagents, materials, analysis tools or data.

Henan Qin; Rui Sun: Analyzed and interpreted the data.

Zhen Ning; Aman Wang: Conceived and designed the experiments; Wrote the paper.

### Data availability statement

Data will be made available on request.

### Declaration of interest's statement

The authors declare no conflict of interest.

### Additional information

Supplementary content related to this article has been published online at https://doi.org/10.1016/j.heliyon.2022.e10116.

## References

[1] R. Siegel, K. Miller, H. Fuchs, A. Jemal, Cancer statistics, 2021, CA Cancer J. Clin. 71 (2021) 7–33.

[2] K. Baumas, J. Soudet, M. Caizergues-Ferrer, M. Faubladier, Y. Henry, A. Mougin, Human RioK3 is a novel component of cytoplasmic pre-40S pre-ribosomal particles, RNA Biol. 9 (2012) 162–174.

[3] Y. Shen, K. Tang, D. Chen, M. Hong, F. Sun, S. Wang, Y. Ke, T. Wu, R. Sun, J. Qian, Y. Du, Riok3 inhibits the antiviral immune response by facilitating TRIM40-mediated RIG-I and MDA5 degradation, Cell Rep. 35 (2021) 109272.

[4] J. Feng, P. De Jesus, V. Su, S. Han, D. Gong, N. Wu, Y. Tian, X. Li, T. Wu, S. Chanda, R. Sun, RIOK3 is an adaptor protein required for IRF3-mediated antiviral type I interferon production, J. Virol. 88 (2014) 7987–7997.

[5] A. Kimmelman, A. Hezel, A. Aguirre, H. Zheng, J. Paik, H. Ying, G. Chu, J. Zhang, E. Sahin, G. Yeo, A. Ponugoti, R. Nabioullin, S. Deroo, S. Yang, X. Wang, J. McGrath, M. Protopopova, E. Ivanova, J. Zhang, B. Feng, M. Tsao, M. Redston, A. Protopopov, Y. Xiao, P. Futreal, W. Hahn, D. Klimstra, L. Chin, R. DePinho, Genomic alterations link Rho family of GTPases to the highly invasive phenotype of pancreas cancer, Proc. Natl. Acad. Sci. U. S. A 105 (2008) 19372–19377.

[6] D. Singleton, P. Rouhi, C. Zois, S. Haider, J. Li, B. Kessler, Y. Cao, A. Harris, Hypoxic regulation of RIOK3 is a major mechanism for cancer cell invasion and metastasis, Oncogene 34 (2015) 4713–4722.

[7] T. Zhang, D. Ji, P. Wang, D. Liang, L. Jin, H. Shi, X. Liu, Q. Meng, R. Yu, S. Gao, The atypical protein kinase RIOK3 contributes to glioma cell proliferation/survival, migration/invasion and the AKT/mTOR signaling pathway, Cancer Lett. 415 (2018) 151–163.

[8] Z. Ning, X. Guo, X. Liu, C. Lu, A. Wang, X. Wang, W. Wang, H. Chen, W. Qin, X. Liu, L. Zhou, C. Ma, J. Du, Z. Lin, H. Luo, W. Otkur, H. Qi, D. Chen, T. Xia, J. Liu, G. Tan, G. Xu, H.-l. Piao, USP22 regulates lipidome accumulation by stabilizing PPARγ in hepatocellular carcinoma, Nat. Commun. 13 (2022).

[9] M. Pereira, A. Santos, D. Gonçalves, A. Cardoso, S. Consonni, F. Gozzo, P. Oliveira, A. Pereira, A. Figueiredo, A. Tiroli-Cepeda, C. Ramos, A. de Thomaz, C. Cesar, K. Franchini, αB-crystallin interacts with and prevents stress-activated proteolysis of focal adhesion kinase by calpain in cardiomyocytes, Nat. Commun. 5 (2014) 5159.

[10] M. Nagano, D. Hoshino, N. Koshikawa, T. Akizawa, M. Seiki, Turnover of focal adhesions and cancer cell migration, Int. J. Cell Biol. 2012 (2012), 310616.

[11] F. Sulzmaier, C. Jean, D. Schlaepfer, FAK in cancer: mechanistic findings and clinical applications, Nature reviews, Cancer 14 (2014) 598–610.

[12] J. Parsons, Focal adhesion kinase: the first ten years, J. Cell Sci. 116 (2003) 1409–1416.

[13] S. Hochwald, C. Nyberg, M. Zheng, D. Zheng, C. Wood, N. Massoll, A. Magis, D. Ostrov, W. Cance, V. Golubovskaya, A novel small molecule inhibitor of FAK decreases growth of human pancreatic cancer, Cell Cycle (Georgetown, Tex.) 8 (2009) 2435–2443.

[14] D. Zheng, V. Golubovskaya, E. Kurenova, C. Wood, N. Massoll, D. Ostrov, W. Cance, S. Hochwald, A novel strategy to inhibit FAK and IGF-1R decreases growth of pancreatic cancer xenografts, Mol. Carcinog. 49 (2010) 200–209.

[15] G. Konstantinidou, G. Ramadori, F. Torti, K. Kangasniemi, R. Ramirez, Y. Cai, C. Behrens, M. Dellinger, R. Brekken, I. Wistuba, A. Heguy, J. Teruya-Feldstein, P. Scaglioni, RHOA-FAK is a required signaling axis for the maintenance of KRAS-driven lung adenocarcinomas, Cancer Discov. 3 (2013) 444–457.

[16] J. Stewart, X. Ma, M. Megison, H. Nabers, W. Cance, E. Kurenova, E. Beierle, Inhibition of FAK and VEGFR-3 binding decreases tumorigenicity in neuroblastoma, Mol. Carcinog. 54 (2015) 9–23.

[17] H. Jiang, S. Hegde, B. Knolhoff, Y. Zhu, J. Herndon, M. Meyer, T. Nywening, W. Hawkins, I. Shapiro, D. Weaver, J. Pachter, A. Wang-Gillam, D. DeNardo, Targeting focal adhesion kinase renders pancreatic cancers responsive to checkpoint immunotherapy, Nat. Med. 22 (2016) 851–860.

[18] R. François, K. Maeng, A. Nawab, F. Kaye, S. Hochwald, M. Zajac-Kaye, Targeting focal adhesion kinase and resistance to mTOR inhibition in pancreatic neuroendocrine tumors, J. Natl. Cancer Inst. 107 (2015).

[19] A. Mohanty, R. Pharaon, A. Nam, S. Salgia, P. Kulkarni, E. Massarelli, FAK-targeted and combination therapies for the treatment of cancer: an overview of phase I and II clinical trials, Expet Opin. Invest. Drugs 29 (2020) 399–409.